JOURNAL OF PROPULSION AND POWER
Vol. 18, No. 5, September–October 2002

Numerical Simulation of a Pulse Detonation Engine with Hydrogen Fuels

Houshang B. Ebrahimi*
Arnold Engineering Development Center, Arnold Air Force Base, Tennessee 37389
and
Charles L. Merkle†
University of Tennessee Space Institute, Tullahoma, Tennessee 37388

The present computational study explores some issues concerning the operational performance of pulse detonation engines (PDE) with hydrogen/oxygen propellants. One- and two-dimensional, transient calculations are employed assuming finite rate chemical kinetic for hydrogen/oxygen combustion based on eight chemical species and 16 reactions. The CFD model was applied to compute the physical attributes of various global detonation phenomena, including shock speed, pressure spike behaviors, and Chapman–Jouguet detonation conditions. Methods for ensuring detonation initiation in the computations by means of a specified high-pressure shock initiation region are examined and details of initiation at closed and open ends are contrasted. The open-end initiation results help to verify the computational methodology and to gain additional insight into the behavior of the closed-end solutions. The effects of reducing ambient pressure at the exit of the cylinder for multicycle operations are investigated. Two-dimensional calculations were performed to study potential precombustion effects due to cyclic refueling processes in the engine. Results indicate that elevated chamber wall temperatures (approximately 1500 K) simulating multiple cycle heating produce some reactions near the wall without predetonation during the refueling process. Overall, one- and two-dimensional approximations are in reasonable agreement. Thrust and specific impulse are computed for a variety of conditions to give an indication of potential performance of a PDE.

Introduction

PULSED detonation engines (PDEs) have received considerable attention over the past decade for potential airbreathing and rocket propulsion applications.[1–6] The PDE differs from conventional propulsion devices such as gas turbines and chemical rockets in two primary ways. First, it generates thrust intermittently. Second, it produces a significant pressure rise in the combustor. The intermittent character of the engine poses design challenges for the nozzle and inlet, while also raising concern over acoustic signatures. The combustion-generated pressure rise represents one of the primary perceived benefits of a PDE device in that it may reduce compression or pumping requirements. A PDE generates pressure in the combustor by using a detonation rather than a deflagration to burn the fuel. Potential implementations of PDEs encompass both airbreathing and nonairbreathing applications. The airbreathing versions collect air from the surrounding atmosphere to serve as the oxidizer, whereas the nonairbreathing versions carry their oxidizer onboard.

The combustor for a PDE is generally a long, narrow chamber with an open end and a closed end. In operation, this tube is filled with a mixture of fuel and oxidizer, and a detonation is initiated at some location in the tube. The resulting pressure rise in the tube causes the gases to flow out the open end, creating an impulse that can be used to provide thrust. After a fixed time interval during which conditions inside the tube return toward the quiescent state, a set of valves is opened and the tube is again filled, allowing the process to repeat. Although the detonation can be initiated at any point in the tube, it is common to consider locations near either end. In the examples considered herein, the detonation is initiated near the closed end and proceeds toward the open end.

It is convenient to divide the processes occurring in a single cycle of a PDE into three phases: 1) the fill time during which the chamber is filled with reactants, 2) the detonation travel time during which the detonation is initiated and traverses through the chamber consuming the reactants, and 3) the blowdown time during which the bulk of the combustion products are expelled by a system of compression and rarefraction waves. After the blowdown process, the fill process starts again and the cyclic operation continues.

A variety of issues arises in the design and analysis of PDE phenomena. These include 1) the identification of appropriate mechanisms for initiating a sustainable detonation wave, 2) the transition of a deflagration wave to a detonation shock, 3) appropriate propellant fill procedures, 4) heat transfer to the chamber walls during the hot portion of the cycle and the resultant propellant heating before detonation, and 5) acoustic wave levels generated during the engine cycle.

In the present paper, we consider the analysis of PDEs by means of unsteady, time-accurate computational modeling. The results of both one- and two-dimensional computations are presented. Our emphasis is on the propulsive characteristics of the engine and does not focus on the well-known cellular characteristics of the detonation front or on the physics of the detonation-to-deflagration transition. In both the one- and two-dimensional studies, the detonation is treated as an organized front that sweeps through the combustible mixture. As an initiation mechanism, we use a high-pressure, high-temperature "spark" initiation region to start the detonation. As in PDE experiments, it is necessary that this initiation mechanism be sufficient to produce reliable and repeatable detonations. The solutions are sensitive to the volume of this shock-generation region, its location, and its specified temperature and pressure. Means for assuring initiation in the one- and two-dimensional computations are discussed, along with a computational grid sensitivity investigation to set the background for the study. Results are then presented for multicyclic operation, including pulse rates and thrust and specific impulse I_{sp} levels for various conditions. One-dimensional

Received 23 June 2000; revision received 5 April 2002; accepted for publication 7 June 2002.

*Engineer Specialist, Jacobs Sverdrup AEDC Group.
†Professor, Chair in Computational Mechanics, Member, AIAA.

computations are used to estimate the effects of variable backpressure on the operation of the PDE engine. Two-dimensional computations are used to assess the appropriateness of the one-dimensional computations and to estimate the effects of elevated wall temperatures on the refueling process. Throughout the analysis, a stoichiometric mixture of hydrogen and oxygen (representing a commonly used space propulsion combination) is used as propellants.

Computational Methodology

The GPACT computer program[7] was applied to simulate the unsteady detonation phenomena as discussed earlier. The GPACT algorithm solves the three-dimensional, Reynolds-averaged Navier–Stokes equations using the upwind Roe finite volume scheme with Gauss–Seidel line relaxation. In the present work, only one- and two-dimensional geometries were considered.

Numerical Procedure Used to Establish Detonation

An important issue in computational simulations of PDE operation is identifying a reliable numerical method for initiating the detonation. Neither one- nor two-dimensional models mimic the correct physics of detonation initiation, but a method for ensuring that the detonation is established is just as important in numerical simulations as in experimental situations. Because detonations are not always obtained in computations, we briefly describe the method we used to ensure initiation.

Figure 1 depicts a detonation chamber with a closed end on the left and an open end on the right. At the start of the computation, the entire chamber is filled with a mixture of unburned hydrogen and oxygen. To initiate the detonation in the one-dimensional computations, we use a small spark region like that shown in Fig. 1 adjacent to the closed end of the tube. The pressure and temperature in the spark region are initially raised to elevated levels, P_H and T_H, respectively, so that a shock begins propagating to the right into the unburned propellant. Under appropriate conditions, this shock steepens into a Chapman–Jouget (C–J) detonation, which then propagates at constant speed throughout the remainder of the tube, whereas for inappropriate conditions the shock decays. To understand the characteristics of the computational detonation mechanism for H_2/O_2 mixtures, we conducted parametric studies in which we varied the spark initiation pressure P_H and the spark volume (size of high-pressure region). In addition, two different left-end boundary conditions, closed and open ends, were also used to clarify the physics. To prevent combustion in the spark region, the high-pressure gases in this region were converted to gaseous H_2O to approximate completed combustion in this zone.

A representative plot showing Mach number contours in the vicinity of the closed end is shown in Fig. 2 to illustrate the characteristics during a representative detonation initiation. At the interface between the spark region and the unburned gases, an expansion fan propagates toward the closed end, where it is reflected as another expansion. Simultaneously, a shock wave moves to the right, compressing the unburned gases. The shock is followed by the familiar contact surface. After a finite incubation time, the computation predicts (for this case) that combustion starts and rapidly catches up with the shock, steepening it and driving it to the C–J condition. The transition between a shock and a detonation is clearly seen from the slope change of the right-running discontinuity in Fig. 2.

Calculations for four different initial pressure levels, $P_H = 90$, 60, 30, and 20 atm, are summarized in Table 1 for the closed end condition. The three highest pressures led to successful detonation initiation, whereas the lowest (20 atm) did not. Higher spark pressures P_H increase the strength of the initial shock and the probability

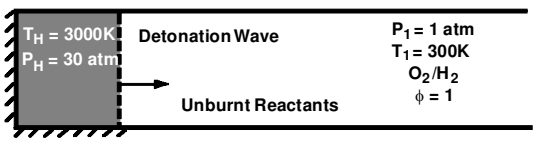

Fig. 1 Schematic of detonation from closed-end cylinder.

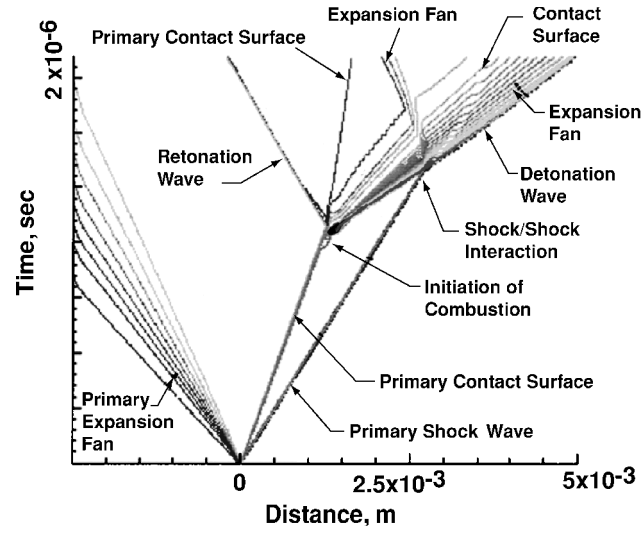

Fig. 2 Detonation shock wave behavior.

of detonation. Table 1 also shows that as P_H is increased from 30 to 90 atm, the distance to the initiation of the detonation decreases (2.6 vs 0.3 mm). An initial pressure and temperature of approximately 30 atm and 3000 K proved sufficient to provide repeatable detonations in the computational solution over multiple cycles for most conditions considered. The axial length of the detonation tube for these detonation initiation studies was set at 0.1 m, a distance sufficient to verify that steady C–J detonations were obtained for cases in which initiation was observed.

The initial shock strength is clearly important to achieving detonation, but the reflected expansion also influences the initiation process. If the reflected expansion overtakes and weakens the shock before combustion is initiated, transition to a detonation is not observed. The interaction between the shock and the expansion is most directly affected by changing the length X_h of the spark region. To test sensitivity to the spark volume, the computation at $P_H = 20$ atm, which did not result in initiation when the initial spark volume was set at 2 mm, was repeated with the spark volume doubled ($X_h = 4$ mm) and increased by a factor of 10 ($X_h = 20$ mm). The spark temperature was maintained at 3000 K. Increasing the length of the spark region increases the time interval during which the shock maintains its original strength, thereby increasing the likelihood of initiation. The computations for both the 4- and 20-mm cases resulted in successful detonations for the 20-atm condition. We also attempted calculations with the spark pressure lowered to $P_H = 10$ atm, but at this pressure detonation did not occur even for the largest spark volume, $X_h = 20$ mm. The lowest detonation pressure obtained for the largest spark volume was 16 atm. These results indicate that threshold levels exist for the combination of spark pressure and spark region volume and that these parameters are important in the simulation of detonation phenomena.

To further understand the role the reflected expansion plays in detonation initiation, we looked for methods to eliminate the reflected expansion. One obvious way is to replace the closed end with an open end at which the expansion reflects as a compression. (This boundary condition was simulated by applying an MOC condition at the left end, effectively implying that the external pressure was initially equal to the pressure in the spark region.) This reflected compression will strengthen the shock as it overtakes it, rather than weakening it. Representative tests with an open end are also summarized in Table 1. For spark conditions corresponding to 30-atm pressure, the distance to detonation initiation was shorter for the open end than the closed end (1 vs 2.6 mm). Similarly, at the 20-atm spark pressure, the open end led to successful detonation, whereas the closed end resulted in failed detonation. These results clearly show that the expansion fan created by the spark initiation region plays a significant role in numerical detonation initiation.

Table 1 Summary of calculation results

Initiation location[a]	Presssure, P_H, atm	P_2/P_1	P_3/P_1	Temperature, T_2, K	X C–J, m	MS_1[b]	MS_2[c]	P_{max}, atm	Detonation occurance
Closed	30	22	8	3450	0.0026	2.9	5.2	35	Yes
Open	30	22	12	3460	0.001	3.1	5.2	26	Yes
Closed	20	——	——	——	——	——	——	——	No
Open	20	22	12	3420	0.001	2.1	5.1	25	Yes
Closed	60	25	9	3450	0.0008	3.3	5.3	30	Yes
Closed	10	——	——	——	——	——	——	——	No
Closed	90	25	11	3450	0.0003	3.6	5.3	32	Yes

[a]Assumed detonation tube length = 0.1 m, constant area. Spark volume filled with gaseous H_2O ($X_H = 0.002$ m). Remaining volume filled with stoichiometric mixture of H_2/O_2.
[b]Shock Mach number before detonation.
[c]Shock Mach number after detonation.

The observations, however, raise an interesting quandary. It is well-known experimentally that detonation initiation at an open end is more difficult than at a closed end, but the present computational results indicate the converse. Although these trends appear contradictory, both are in agreement with physics and serve to provide a more precise understanding of both cases. The difference stems from the manner in which the detonation is initiated. The shock wave generated from the shock-tube-like conditions in the computational solutions will be weakened by the expansion wave reflecting off the closed end. A standard method of characteristics boundary condition that reflects the incoming expansion as a compression will clearly enhance the shock. A closed end diminishes the likelihood of initiation, whereas an open end enhances it. Initiation in experimental situations does not start from an instantaneously imposed finite region of high pressure. In an experiment, the closed end serves to confine the pressure increases created by combustion, thereby strengthening the shock that is created. There is no oppositely directed expansion wave. Similarly, the open end allows the pressure to escape to the external environment. The expansion wave for this condition propagates from left to right, not right to left. External conditions needed in the computation to ensure the opposite reflection boundary condition are different from those typically used in experiments, but the trend shown by the computations is exactly what would be expected from physics and provides a simple means for understanding the impact of the expansion wave in the closed end case.

On the basis of the studies described here, the spark pressure was set to 30 atm, the spark region length to 2 mm, and the closed boundary condition was used for the remainder of the computations. These initiation conditions resulted in repeatable detonation behavior both in single-shot and multicyclic operation. Isolated computations on extremely fine grids (see next paragraph) indicated a weak dependence on grid refinement, but the present initiation limits continued to produce detonation until the solutions were well beyond the grid-independent level. Consequently, these thresholds were not changed to accommodate this weak grid effect.

Overview of the Pulsed Detonation Cycle

Once the detonation is established, it moves throughout the entire tube and exhausts through the open end. The pressure profile in the chamber during this time takes the characteristic shape given in Fig. 3. The pressure rises across the shock and drops slightly during the combustion process. Because the velocity must be zero at the closed end of the chamber, an expansion region is created between the closed end wall and the moving detonation. These rarefaction waves that reflect off the closed end of the chamber trail the generated shock front and cause the pressure to decrease toward a minimum at the wall. The existence of the C–J condition at the detonation ensures that they do not overtake and weaken the shock. As a result, the detonation moves at constant velocity after it is established.

A simulation of the transient detonation process involving a stoichiometric hydrogen/oxygen mixture was performed to provide a preliminary assessment of the numerical model for PDE operational performance analysis. The detonation chamber was modeled as a

Table 2 Detonation properties

Parameter	Calculated	Experiment[a]
U_S, m/s[a]	2840	2820
P_2, atm	21.0	——
T_2, K	3450	——
M_S, Shock Mach number	5.25	——

[a]After detonation.

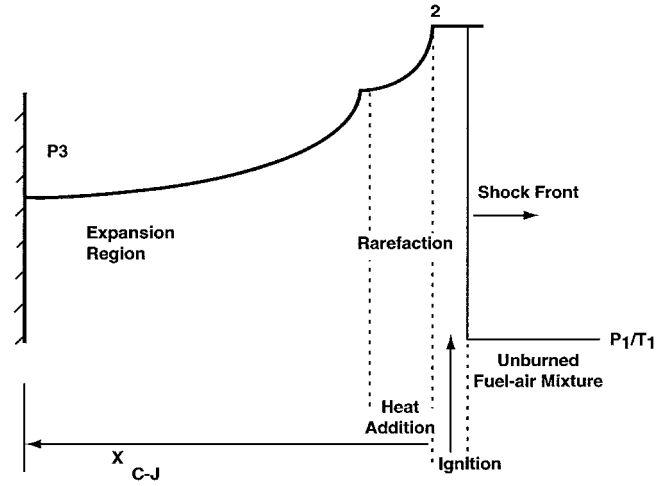

Fig. 3 Pressure distribution behavior of detonation.

cylindrical tube with axial lengths of 0.1 and 0.2 m. A schematic of the detonation process initiated from the closed end of the detonation chamber was shown earlier in Fig. 1. To initialize the computation, a stoichiometric hydrogen/oxygen mixture at 1-atm pressure and 300-K temperature (P_1 and T_1, respectively) was assumed to be at rest within the detonation chamber. A shock wave was initiated from the closed end of the chamber by setting the pressure and temperature in the spark region to $P_H = 30$ atm and $T_H = 3000$ K for most cases. Except where noted, the spark region was taken as 0.2 mm in axial length and included 20 computational grid points. The remaining grid points (1800) were equally spaced in the unburned, downstream region of the detonation tube. Calculated results showing representative parameters for one particular case are presented in Table 2. Also included in Table 2 is a measured shock speed resulting from an experiment conducted[8] at the same conditions as the simulation. The comparison of the measured and calculated shock speed is very close, indicating a reasonably accurate model. For multicyclic operation, the incoming fuel for successive cycles is set to 300 K, whereas the pressure level is determined by the solution. The ambient pressure outside the detonation tube is taken as 1 atm for most of the computations and as 0.1 atm for the remainder.

One-dimensional pressure profiles along the length of the detonation tube at several instances in time are shown in Fig. 4 for the calculation listed in Table 2. Detailed analysis of the results shows that the high-pressure spike that occurs at approximately 0.001 m is indicative of the initiation of the detonation in the one-dimensional

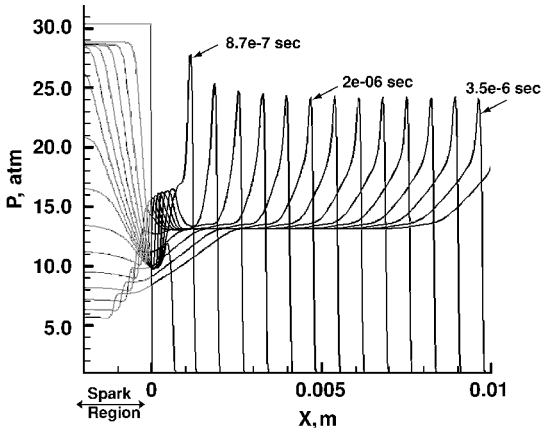

Fig. 4 One-dimensional pressure profile along length of cylinder.

computation. Following initiation, the peak pressure monotonically decreases to a steady value corresponding to a constant velocity detonation. The simulation predicts that the shock propagation speed reaches a constant speed at a location of approximately 2 mm for this case. Before the initiation of the detonation, the shock speed from the spark region propagated at a Mach number of 2.9. After the detonation was established, the detonation accelerated to $M = 5.25$. The simulation also confirms that the burned gas mixture leaves the detonation front at sonic speed relative to the gas condition. As seen in Fig. 4, the peak pressure in the detonation wave, P_1, is predicted to be approximately 22 atm. Because this case was initiated at 1 atm, this corresponds to a pressure ratio across the detonation of $P_2/P_1 = 22$. Because of the expansion in this region and the reflection of the expansion wave off the closed end of the chamber, the pressure in the expansion region, P_3, is lower than the pressure behind the detonation wave. This pressure ratio, P_3/P_1, is approximately 9. It is this P_3/P_1 pressure rise that is useful for producing thrust. This detonation-induced pressure rise is absent in conventional propulsion devices.

Computational Grid Sensitivity Studies

To assess computational grid sensitivity issues for simulating detonation phenomena, five parametric one-dimensional calculations were performed using different uniform grid spacings: $dx = 2.0$, 0.8, 0.4, 0.2, and 0.1 mm. All other initial conditions were held constant. The ignition spark region length was specified as $X_h = 0.02$ m for these cases, and the thermodynamic parameters were set to $T_H = 3000$ K and $P_H = 30$ atm.

In the coarsest grid case ($dx = 2.0$ mm), the correct detonation velocity was predicted within 10%, but the overshoot pressure was considerably lower than those obtained with the other grids, indicating that this grid was near (or slightly beyond) the limit of acceptable resolution. All other grids except the finest predicted consistently accurate detonation speeds and pressure rise. The computation on the finest grid failed to initiate a detonation. Overall, the grid sensitivity studies indicate that reliable one-dimensional solutions can be obtained for a variety of grid sizes, although grid resolution must be carefully assessed in detonation simulations.

Multicycle Effects

The operation of a PDE is composed of several interacting facets. In starting the cycle, the detonation chamber must first be filled with a well-mixed charge of fuel and oxidizer. The detonation must be initiated and allowed to propagate through the chamber. Following this, a reasonable blowdown time must be allowed, after which the propellant fill phase is repeated. Of these several phases, the ones generally requiring the largest portion of the cycle time are the blowdown and fill processes. These two phenomena have a major impact on the engine's pulse repetition and its eventual thrust level. In general, the operation of a PDE must be assessed on the basis of multicyclic operation, wherein a periodic (or quasi-periodic) operation is obtained.

Table 3 Thrust calculation[a,b]

Cycle number	Thrust, N (closed end)	Specific impulse, I_{sp}
1	155.3	251.6
2	138.9	225.1
3	137.0	221.9
4	135.8	220.0
1	182.0	295.0
2	164.3	266.3

[a]Ambient pressure = 1 atm. [b]Cylinder length = 0.2 m.

To identify characteristic features of multicycle operation, the one-dimensional transient model was applied to the closed/open chamber design. As in the earlier computations, the detonation process was initiated in a stoichiometric hydrogen/oxygen mixture with an initial spark pressure and temperature (P_H and T_H) equal to 30 atm and 3000 K, respectively. The velocity in the tube during the first cycle was set to zero, and the pressure was uniform and equal to 10 atm. The length of the initiation region X_H was 0.2 mm and consisted of the first 20 of 1800 computational nodes. A tube length of 0.2 m was specified. The multicycle operation sequence is summarized as follows:

1) The detonation wave is generated and propagates through the combustion cylinder at supersonic speed.

2) The detonation wave exits the engine, and the series of rarefaction waves generated by the detonation propagate upstream into the closed end of the chamber and push the burned gases toward the exit of the chamber.

3) At the closed end of the tube, the pressure eventually decays to ambient levels so that the impulse falls to zero (and can become negative), and velocity throughout the entire tube approaches zero. This is the terminal condition of the first cycle. At these conditions, the cycle at the preceding conditions requires approximately 0.0025 s for a 0.2-m-long tube.

4) At this point, the valves on the closed end of the chamber are opened to allow the chamber to be recharged with fresh fuel and oxidizer. Typical fuel injection velocities were approximately 200 m/s, resulting in refueling times of approximately 0.001 s.

5) As for the blowdown process, the time required for the refueling process is a function of the PDE length and the velocity at which the gaseous mixture is injected into the engine.

Table 3 shows thrust and specific impulse predictions for four pulse detonation operation cycles. The multicycle engine calculations indicate that nearly periodic operation is achieved by the end of the third cycle.

Effects of Ambient Pressure

One possible application for pulsed detonation rocket engines is as an upper-stage propulsion system for space flight. For such applications, an issue of interest is the dependence of PDE performance on the ambient pressure P_{amb}. The implications of operating a PDE at low ambient pressures are of particular interest.

To study the effect of ambient pressure on the characteristics of the PDE operation and on its performance, two calculations were computed for ambient backpressures of 1.0 and 0.1 atm. Apart from the ambient pressure, all other conditions were the same in the two computations. Note that the lower backpressure case was only continued for two cycles. Figure 5 shows Mach number contours of the first cycle for the 0.1-atm case. Note that, for this first pulse, the tube was not exposed to the exit pressure until the first detonation arrived at the exit. A similar cycle time was used for the 0.1-atm case as for the 1.0-atm case. A major difference between this low-pressure case and the 1-atm case is that the low backpressure causes the exit of the tube to remain choked throughout the entire cycle except during the refueling process. This is clearly seen from the Mach number time history at the exit of the tube for the 0.1-atm case, as shown in Fig. 6. By contrast, the 1.0-atm backpressure case not only unchoked at the exit plane, but exhibited a short interval of backflow from the atmosphere into the detonation chamber. This choked exit

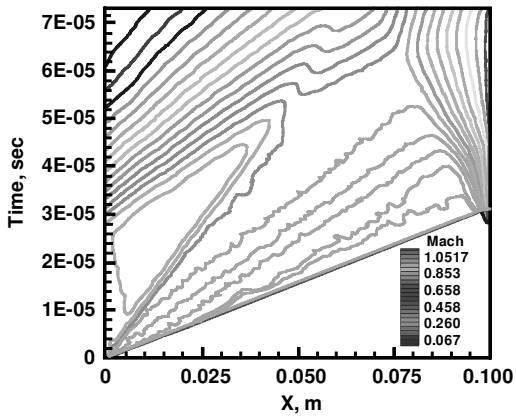

Fig. 5 Mach number contours at $P_{amb} = 0.1$ atm.

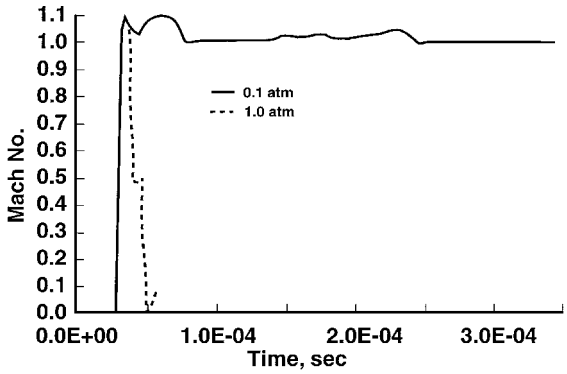

Fig. 6 Mach number time history at exit of the cylinder for $P_{amb} = 0.1$ and 1.0 atm.

implies that the chamber pressure can be kept at pressure levels near those obtained at 1-atm conditions. The choked exit also implies that fuel can be lost out of the exit before the arrival of the detonation, so that very careful valve timing is necessary to maximize engine performance.

The thrust and I_{sp} performance comparison between ambient pressure (1.0 atm) and 0.1 atm at the cylinder exit indicates about a 16% thrust increase at the lower pressure. Table 3 shows time-averaged thrust values at the closed end (thrust) of the tube for four cycles assuming ambient pressures equal to 1.0 atm and for two cycles for ambient pressure equal to 0.1 atm.

Two-Dimensional Effects

As a logical extension of the one-dimensional studies just discussed, two-dimensional simulations were completed at conditions identical to the one-dimensional simulations. For the two-dimensional assessments, the radius of the tube was specified as 0.02 m and the axial extent was again specified as 0.2 m. Three two-dimensional calculations were performed to assess the effect of the initial starting profile conditions on the detonation behavior. The first solution assumed uniform starting conditions, $P_H = 30$ atm and $T_H = 3000$ K, identical to the one-dimensional case, except that a complete two-dimensional solution procedure was applied. The second case assumed a semicircular profile in the spark initiation region to test the effects of non-one-dimensional spark initiation. Overall, the two-dimensional results were in quite close agreement with the one-dimensional results except for the very earliest times in the cycle. The localized detonation initiation in the two-dimensional calculation created a lower pressure on the head end of the chamber for the first 50 μs of the cycle. Figure 7 shows the averaged pressure histories for the two cases during this initial time. As can be seen, the pressure-time traces for the two computations rapidly approach each other and, for times beyond those shown in Fig. 7, remain very similar. This initial difference had almost no effect on the net impulse generated during the cycle.

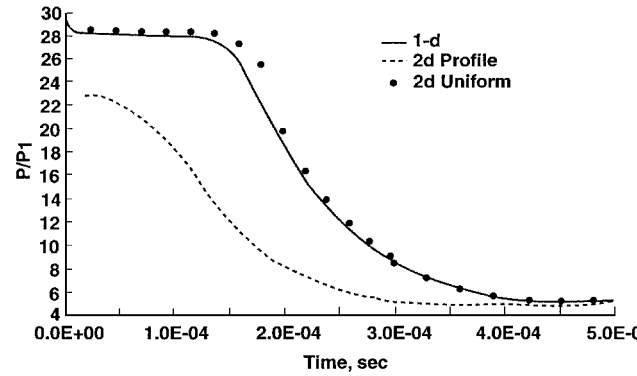

Fig. 7 Pressure profile comparison at closed end.

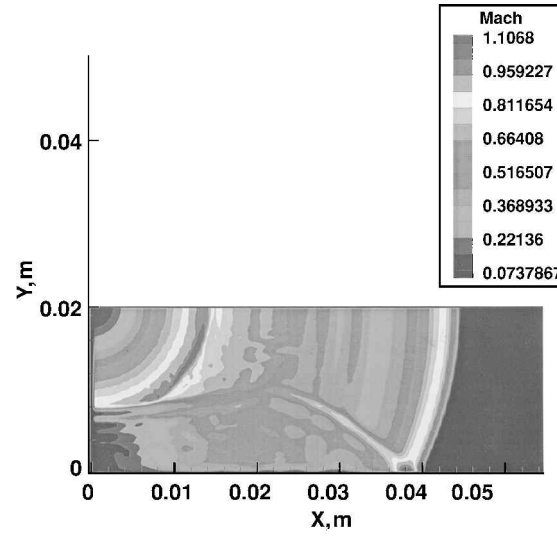

Fig. 8 Mach number contours of a two-dimensional calculation with two-dimensional initial profile: a) O_2 and b) H_2O.

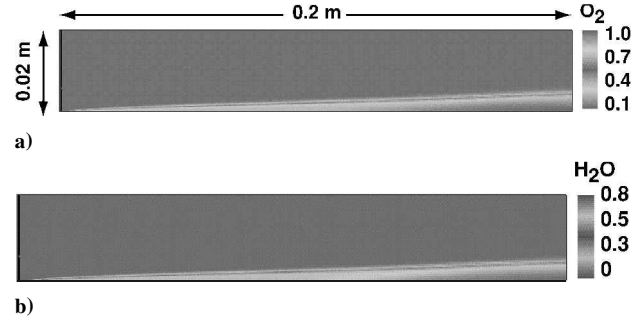

Fig. 9 Mass fraction contours during refueling process.

Mach number contours resulting from the semicircular start conditions are shown in Fig. 8. The reflection of the shock wave is clearly visible near 0.04 m, but as the shock propagates down the tube, it rapidly assumes a one-dimensional shape. Again, these results indicate that one- and two-dimensional solutions remain similar even when different starting conditions are used.

The third two-dimensional case was similar to the other two, except that the left end was open to allow fuel filling, and the wall temperature was set to 1500 K. The purpose of this computation was to assess the effects of cyclic heating on the fresh propellant charge and its potential influence on the fuel combustion before detonation initiation. The temperature and velocity of the fresh fuel and oxidizer were specified as 300 K and 400 m/s, respectively. Figures 9a and 9b show H_2O and O_2 mass fraction contours during the refueling process. As the fuel flows along the hot wall, the temperature in the boundary layer rises above that of the wall, indicating that some

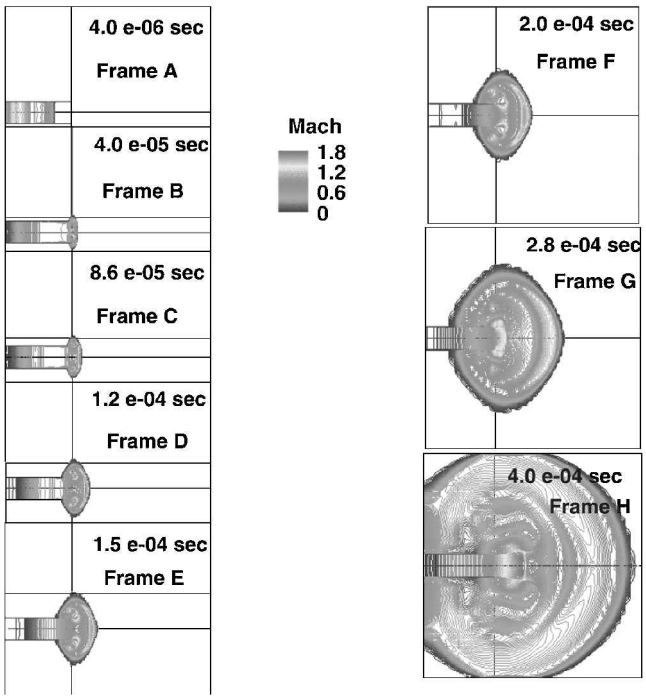

Fig. 10 Time history of Mach number contours with viscous and finite rate chemistry calculations.

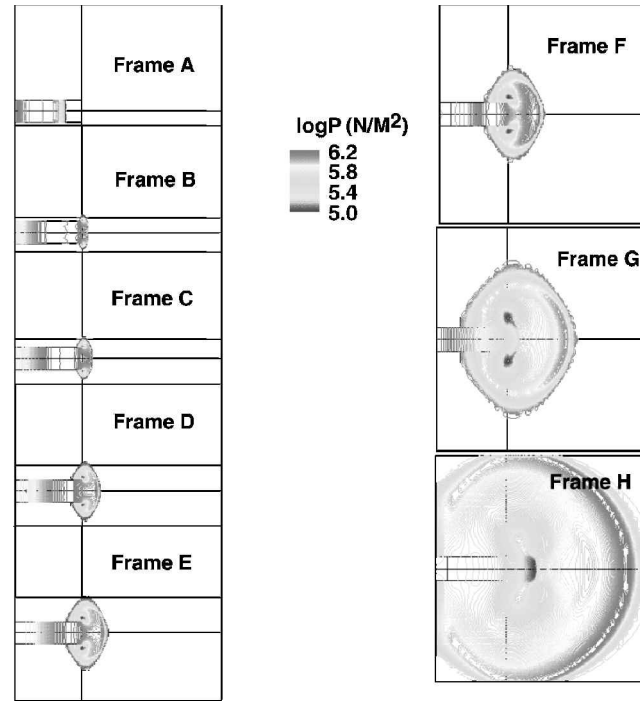

Fig. 11 Time history of pressure contours with viscous and finite rate chemistry calculations.

reaction is taking place. (Similar computations assuming frozen flow verified that the maximum temperature inside the flowing gases remained below the wall temperature, as it should.) In addition, the species profiles show that the water mass fraction has reached 0.84 near the wall. We emphasize that these wall-heating effects represent only a few calculations, not an in-depth study, and that they are for a relatively short tube; however, overall, they indicate that the hot chamber does not ignite the incoming fresh propellants. Again, longer time computations are needed to assess how rapidly this hot spot near the wall propagates.

Figures 10 and 11 show Mach number and log of the pressure contours for a sequence of eight times in a two-dimensional computation aimed at understanding the importance of multidimensional effects at the open end of a PDE. The computation corresponds to an initial pulse where the gas inside the tube in front of the detonation, as well as the gas outside the tube, is initially quiescent. In the periodic case, the flow inside the tube would have residual motion and pressure gradients from the preceding pulse, and the environment outside the tube would also contain disturbances. The results from this initial computation are, however, quite interesting, and the simpler flowfield makes the events easier to interpret. In each plot, the Mach number contours inside the detonation tube, as well as the disturbances surrounding the exit of the tube, are shown in the main part of Figs. 10 and 11.

The first plot in frame A of Figs. 10 and 11 shows Mach number and log of the pressure before the detonation has reached the end of the open tube local Mach number at the shock wave is sonic.

In the second part (frame B) of Figs. 10 and 11, the Mach number distribution is given just after the detonation has emerged from the tube. Because the ambient gas is pure air, the detonation transitions to a shock wave as it moves outside the tube. The gases behind the detonation are expanding around the top and bottom edges of the tube in nearly cylindrical fashion, but the remainder of the shock front is nearly planar in shape. The Mach number at the exit plan reaches the sonic velocity in a very small region near the upper and lower corners, where the flow is essentially expanding in shock-tube fashion.

In the third (frame C) and fourth (frame D) plots the external shock has progressed about a one- and two-tube radii away from the exit plane. Key issues here are the very small cylindrical sonic regions near the corners, but subsonic flow elsewhere. It is also clear that the shock is traveling forward along the outside of the tube. The essentially planar shock shape in frame A is now approaching a cylindrical shape. As the shock distance becomes much larger than the tube diameter, the external shock appears more and more like a shock created from a point source.

In frame E and frame F, the shock has traveled approximately three and four radii past the exit plane. Note that it has propagated a similar distance in the directions normal to the tube and back upstream along the outer surface. Again, note that the Mach number at the exit plane remains subsonic across the entire duct. There are two supersonic regions on the centerline, but they are both downstream of the exit plane. The corresponding pressure plot (not shown) indicates that the entire tube and all of the gas inside the shock is at a pressure that is substantially above ambient (around 6 atm). It is the presence of this high pressure outside the tube that keeps the outflow subsonic. The corresponding one-dimensional results would give choked flow at the exit almost as soon as the shock exits the tube. We note, however, that the present plot (and, indeed, the entire sequence) is very early in time in terms of a full PDE cycle.

As time increases, the shock continues to propagate outward. The pressure immediately behind the shock decreases slowly with time as the shock weakens because of the two-dimensional expansion, but the pressure near the exit plane decreases rapidly. Representative Mach number contours for a time at which the shock has traveled about five radii are given in frame G. At this time, the pressure outside the exit has decreased to approximately 2 atm, but the outflow remains subsonic. Nevertheless, the Mach number at the exit plane is increasing slowly. The Mach number on the centerline shows very strong axial gradients resulting from the cylindrically expanding shock wave. Note that the region of the flowfield shown in the plot is much smaller than the computational domain.

The final frame given in Figs. 10 and 11 again shows subsonic flow at the exit plane, but in the interim between frames G and H, the exit flow has gone supersonic (to about $M = 1.2$) across the entire duct exit plane. It is now rapidly decreasing, and presumably will soon reach inflow conditions. The pressure at the exit plane of the tube has actually decreased below ambient pressure, but the flow remains outward because the pressure outside the tube is even further below ambient. Also note that, at this time, the external shock has propagated all of the way to the upstream end of the tube, and there is a wide zone of flow going in the upstream direction. This external flow will gradually decay, but significant disturbances will most certainly remain beyond the time for the next PDE pulse. This will

result in detailed changes in the interaction between the external tube and the external environment. The external domain needed to extend the present computations to multiple pulses, however, becomes prohibitively large because the present computation ends after approximately 1% an entire cycle. Additional computations are in progress to evaluate later times and to compare these results with one-dimensional computations for both first-pulse and periodic conditions.

Summary

A series of transient simulations of H_2/O_2 detonation processes in PDEs was completed using the GPACT CFD computer model. The intent of these calculations was to assess the capabilities of CFD models to capture realistic trends for transient detonation analyses and to predict representative performance levels for a PDE system. An H_2/O_2 chemical system comprising eight chemical species (O, O_2, OH, H, HO_2, H_2O, H_2O_2, and H_2) and 16 reactions was used. A single quantitative comparison of a measured shock velocity with the shock velocity predicted by the GPACT model was reasonable. The calculations realistically captured the relative conditions in the flow regions created by the propagating shock and the subsequent detonation. The solutions required approximately 12 h for each case to complete on an SGI Octane workstation.

The numerical detonation process was initiated by means of a high temperature and pressure region adjacent to the end of the tube. The results indicated that threshold levels existed below which initiation could not be obtained. Higher initiation pressures led to shorter transition distances, whereas lower pressures failed to initiate a detonation. The initial limitation appeared to arise from shock weakening by the rarefaction following the detonation. This was verified by open end calculations in which the approaching rarefaction was forced to reflect as a compression. Increasing the spark region volume improves the liklihood of detonation occurrence at low P_H conditions.

The effect of the computational mesh spacing was shown to be relatively insignificant within a range of grid spacings, but did show variations in sensitivity for both very coarse grids and very fine grids. The effect of ambient pressure was also investigated. When the ambient pressure was reduced from 1.0 to 0.1 atm, the exit plane remained choked throughout the cycle, and the thrust was increased by about 15%.

Computations of multiple-pulse engine cycles typically showed that periodic conditions were obtained after the second cycle. Multicycle simulation is imperative for low-backpressure cases because the pressure level in the tube cannot be specified in advance, but is determined by the periodic operation. In addition to these one-dimensional results, several multidimensional phenomena were assessed.

Contrasting one- and two-dimensional approximations indicate that two-dimensional starting profiles have little downstream effect on the detonation characteristics and that the shock structure and detonation behavior are similar to their one-dimensional counterparts. Two-dimensional initiation changed the head-end pressure for very short times, but after the detonation has traveled about one tube diameter, the two-dimensional solutions behave much like their corresponding one-dimensional counterparts. The impact of hot chamber walls on premature propellant ignition was also investigated, but was found to be relatively benign for the conditions evaluated. Finally, two-dimensional effects at the exit plane were simulated by incorporating a large external grid to capture the transmitted shock. The external shock initially increases the pressure at the exit plane such that the outflow remains subsonic, even though the pressure at the exit plane is several times the ambient pressure. At intermediate times, this same shock drops the pressure below the ambient value, postponing the time at which inflow begins. These initial results suggest a multidimensional end correction may help to improve the fidelity of one-dimensional simulations of PDEs.

Acknowledgments

This investigation was supported by NASA Marshall under contract NAS8-97301. The research reported herein was performed by the Arnold Engineering Development Center (AEDC), Air Force Materiel Command. Work and analysis for this research were performed by personnel of Jacobs Sverdrup AEDC Group, technical services contractor for AEDC.

References

[1]Sideman, S., and Grossman, W., "Pulsed Detonation Engine Experimental and Theoretical Review," AIAA Paper 92-3168, Jan. 1992.

[2]Bussing, T., and Pappas, G., "Pulse Detonation Engine," AIAA Paper 95-2577, July 1995.

[3]Lynch, D., Edelman, R., and Palaniswamy, S., "Computational Fluid Dynamics Analysis of the Pulse Detonation Engine Concept," AIAA Paper 94-0264, Jan. 1994.

[4]Cambier, J. L., and Tegner, J. K., "Strategies for Pulsed Detonation Engine Performance Optimization," *Journal of Propulsion and Power*, Vol. 14, No. 4, 1998, pp. 489–498.

[5]Kailasanath, K., "Review of Propulsion Applications of Detonation Waves," *AIAA Journal*, Vol. 38, No. 9, 2000, pp. 1698–1708.

[6]Ebrahimi, H., Mohanraj, R., and Merkle, C. L., "Multilevel Analysis of Pulsed Detonation Engines," AIAA Paper 2000-3589, July 2000.

[7]Ebrahimi, H., "Numerical Simulation of Transient Jet-Interaction Phenomenology in a Supersonic Freestream" *Journal of Spacecraft and Rockets*, Vol. 37, No. 6, 2000, pp. 713–719.

[8]Soloukhin, R. I., *Shock Waves and Detonations in Gases*, Mono Book, Baltimore, MD, 1966.